Conformational Analysis of TMC114, a Novel HIV-1 Protease Inhibitor

Kanda Nivesanond,[†] Anik Peeters,[‡] Dirk Lamoen,[§] and Christian Van Alsenoy*[,†]

Department of Chemistry, University of Antwerp, Drie Eiken Campus, B-2610 Antwerp, Belgium, Tibotec BVBA, Gen. De Wittelaan L 11B 3, B-2800 Mechelen, Belgium, and Department of Physics, University of Antwerp, Middelheim Campus, B-2020 Antwerp, Belgium

Received April 11, 2007

TMC114, a potent novel HIV-1 protease inhibitor, remains active against a broad spectrum of mutant viruses. In order to bind to a variety of mutants, the compound needs to make strong, preferably backbone, interactions and have enough conformational flexibility to adapt to the changing geometry of the active site. The conformational analysis of TMC114 in the gas phase yielded 43 conformers in which five types of intramolecular H-bond interactions could be observed. All 43 conformers were subject to both rigid and flexible ligand docking in the wild-type and a triple mutant (L63P/V82T/I84V) of HIV-1 protease. The largest binding energy was calculated for the conformations that are close to the conformation observed in the X-ray complexes of TMC114 and HIV-1 protease.

INTRODUCTION

The human immunodeficiency virus type-1 aspartyl protease (HIV-1 PR) is one of the major targets for antiretroviral therapy.[1−3] HIV-1 PR has become the major target in the rational design of drugs for the treatment of AIDS, as can be seen from the literature, in which a large number of computational studies have been performed.[4−13] A significant number of compounds which are highly potent HIV-1 PR inhibitors (PIs) has been developed.[14−22] However, the need to develop better drug candidates is an ongoing effort due to the ability of the protease to mutate into drug-resistant forms.[23] The PIs currently on the market cannot be considered as having a broad spectrum because their average activity against a panel of resistant mutants is more than 1 log lower than their wild-type activity (10-fold decrease in activity on the mutants with respect to the wild-type virus).[24] Therefore, novel inhibitors need to be more active against resistant variants of HIV-1. Consequently, a novel protease inhibitor TMC114 (Figure 1a) has been developed.[24] TMC114 is chemically related to TMC126 (Figure 1b), but TMC126 lacked sufficient druglike properties such as solubility, metabolic stability, and oral absorption to be a viable lead.[25] TMC114 is extremely potent against a wide spectrum of HIV strains in vitro, including a variety of multiprotease inhibitor-resistant clinical strains. The stereochemistry of the bis-tetrahydrofurane (bis-THF) moiety in TMC114 has been shown to be of major importance for the resulting biological activity because the two bis-THF oxygen atoms accept hydrogen bonds from the Asp29 and Asp30 backbone N−H functions.[24] In addition to these important intermolecular interactions, the compound needs to be able to adopt different conformations to fit in the binding pockets of the various mutants.

To study the conformational flexibility of molecules a variety of efficient conformational searching methods are available: simulated annealing,[26−28] Monte Carlo,[29−34] and eigenvector following algorithms.[35−37] A number of methodologies for binding free energy calculations have also been developed.[38−43] In this work, the Monte Carlo (MC) search method and quantum mechanical (QM) calculations were used for the conformational study of TMC114 in the gas phase. In order to find the conformation that fits best into the binding pocket of HIV-1 PR, the lowest energy conformations from the gas-phase calculations were also docked into the binding site of the wild-type and a triple mutant (L63P/V82T/I84V) of HIV-1 PR. This was done using both a rigid and flexible ligand docking algorithm. The results are compared to the X-ray structures of TMC114 complexed to wild-type and triple mutant HIV-1 PR respectively.

METHODS

1. Conformational Searches. The Monte Carlo search method and quantum mechanical calculations were used to study the conformational space of TMC114. The Monte Carlo search method was performed using Accelrys software (Cerius2 and InsightII programs). The quantum mechanical calculations were performed at the Hartree−Fock (HF) level with the 6-31G** basis set[44−45] using the BRABO[46] program.

In the first step, five Monte Carlo (MC) simulations were started from the X-ray structure of TMC114 bound to HIV-1 PR (PDB code 1T3R)[25] using the cff1.01 force field with the Boltzmann jump search method as implemented in Cerius2. Each simulation generated 500 conformations. After each MC run, all 500 conformations were clustered based on the root-mean-square deviation (rmsd) of their torsion angles, the lowest energy conformation of each cluster was minimized, and then these minimized structures were re-clustered. In the next step, a full energy minimization was performed in InsightII using a Discover force field and the VA09A minimization procedure for the lowest energy conformer of each new cluster. Finally, the conformations

* Corresponding author phone: +32-3-820-2366; fax: +32-3-820-2310; e-mail: kris.vanalsenoy@ua.ac.be.
[†] Department of Chemistry, University of Antwerp.
[‡] Tibotec BVBA.
[§] Department of Physics, University of Antwerp.

10.1021/ci7001318 CCC: $40.75
Published on Web 01/04/2008

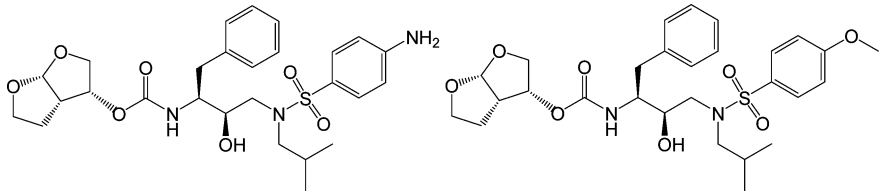

(a) (b)

Figure 1. 2D structure of TMC114 (a) and TMC126 (b).

Table 1. Single Point Energy of All Conformers Divided into 4 Groups

group	no. of conformers	name	relative single point energy (kcal/mol)
1	16	conf01 - conf16	$0.000^a \leq E < 3.139$
2	13	conf17 - conf29	$3.139 < E < 4.395$
3	14	conf30 - conf43	$4.395 < E < 5.651$
4	260	conf44 - conf303	$E > 5.651$

[a] Compared to the lowest energy conformer, conf01 (−2128.805 Hartree).

obtained in this way for each of the five MC simulations were collected and superimposed, and similar conformers were removed.

In the second step, single point energy calculations of the conformers that were obtained from the MC search were performed at the HF/6-31G** level using BRABO. The compounds were ranked by this calculated single point energy and numbered accordingly. In the next step, the lowest single point energy conformers were selected for a complete geometry optimization at the HF/6-31G** level. For reason of comparison, the experimental wild-type X-ray structure named "confwt" was also optimized and compared with all calculated conformers.

The free energy of solvation (ΔG) of the 43 selected conformers has been computed with the polarizable continuum model (PCM)[47] using ab initio molecular orbital calculations at the Hartree−Fock (HF) level with the 6-31G** basis set by Gaussian 03. The van der Waals surface and the water accessible surface have been calculated using the VEGA program.[48]

2. Autodock Calculations. Two high-resolution X-ray structures are available for the complex of TMC114 and HIV-1 PR, one with the wild-type protein (PDB code 1T3R) and one with a triple mutant (L63P/V82T/I84V; PDB code 1T7I).[25] Docking calculations were carried out using AutoDock 3.0.[49] AutoTors[49] was used to define the torsions of the inhibitor for the docking algorithm. A 3D grid with 60 × 54 × 60 points and a spacing of 0.375 Å was created by AutoGrid[49] to evaluate the binding energies between the inhibitor and the enzyme. Kollman-united-atom[50] and MMFF94[51] atomic charges were used for HIV-1 PR and TMC114, respectively. In this study, the water molecule in the flap region of HIV-1 PR was included in the calculations. Three binding energy terms were taken into account in the docking step: the van der Waals interaction represented as a Lennard-Jones 6−12 dispersion/repulsion term, the hydrogen-bonding represented as a directional 10−12 term, and the Coulombic electrostatic potential. The Lamarckian Genetic Algorithm (LGA) and the pseudo-Solis and Wets methods were applied for minimization.

Docking started with the population of previously calculated conformations in random orientations and at random translations. Translations were set to have a maximum limit of 2 Å/step, and the orientation step size for the angular component and the torsions had a maximum limit at 50 degrees/step. In this study, all 15 torsions of TMC114 were released for flexible ligand docking, and all torsions were

Table 2. Relative Energy after Full Geometry Optimization (Compared to conf17), Intramolecular H-Bond Interaction Types, RMSD (Compared to the Optimized X-ray Structure), van der Waals Surface, and Free Energy of Solvation of 43 Optimized Conformers of TMC114

	rel E^a (kcal/mol)	intramolecular H-bond no.	rmsd[b] (Å)	VDW surface (Å)	ΔG solvation (kcal/mol)	total E (kcal/mol)
conf43	8.32	1	5.19	583.9	−7.40	0.92
confwt	7.05	0	0.00	592.7	−15.43	−8.38
conf42	6.62	1	4.57	587.3	−11.83	−5.21
conf41	6.16	1	4.87	587.9	−10.51	−4.35
conf40	6.14	1	2.25	585.4	−11.85	−5.71
conf39	6.12	2,4	3.32	582.1	−9.60	−3.48
conf38	5.95	0	3.18	595.1	−11.84	−5.89
conf29	5.86	3	3.74	588.3	−11.19	−5.33
conf37	5.81	0	2.96	590.3	−11.19	−5.38
conf36	5.69	1	3.01	586.5	−11.76	−6.07
conf35	5.48	0	1.88	593.1	−11.76	−6.28
conf28	5.25	1	4.26	586.6	−12.59	−7.34
conf34	5.04	0	3.33	593.3	−10.70	−5.66
conf33	5.01	0	3.35	590.4	−10.74	−5.73
conf32	4.95	1	2.53	585.7	−12.00	−7.05
conf27	4.89	2	3.60	588.4	−14.33	−9.44
conf26	4.77	3	5.14	584.1	−7.14	−2.37
conf16	4.74	2	3.07	588.1	−12.25	−7.51
conf15	4.66	5	5.37	586.0	−5.50	−0.84
conf14	4.31	1	5.33	588.6	−7.03	−2.72
conf13	4.27	0	1.77	588.3	−9.89	−5.62
conf25	4.14	1	2.71	585.7	−7.34	−3.20
conf24	4.03	1,5	5.09	583.3	−9.84	−5.81
conf12	3.79	3	5.20	588.0	−8.04	−4.25
conf31	3.68	1	2.40	584.4	−11.48	−7.80
conf30	3.67	1	2.67	588.2	−11.49	−7.82
conf23	3.54	2	2.82	586.9	−12.47	−8.93
conf22	3.39	1	3.11	589.0	−14.32	−10.93
conf21	3.08	0	4.86	588.5	−8.79	−5.71
conf11	2.90	1	2.11	589.7	−12.43	−9.53
conf20	2.78	0	4.54	594.2	−10.24	−7.46
conf10	2.72	1	2.55	594.3	−10.71	−7.99
conf09	2.68	1	3.52	594.7	−11.31	−8.63
conf08	2.65	1	3.12	589.5	−14.56	−11.91
conf19	2.51	1	2.87	589.9	−14.19	−11.68
conf18	2.49	1	2.87	586.6	−14.19	−11.70
conf07	2.37	3	5.14	593.5	−7.06	−4.69
conf06	2.19	3	4.95	586.0	−6.42	−4.23
conf05	2.07	1	1.97	588.4	−13.34	−11.27
conf04	1.92	5	4.63	591.3	−8.84	−6.92
conf03	1.84	1	2.89	589.2	−12.42	−10.58
conf02	1.56	1	3.16	580.5	−11.24	−9.68
conf01	0.27	1	3.70	588.2	−8.08	−7.81
conf17	0	5	4.76	585.3	−8.09	−8.09

[a] Compared to conf17, the lowest energy conformer. [b] Compared to the optimized X-ray structure of TMC114 (confwt).

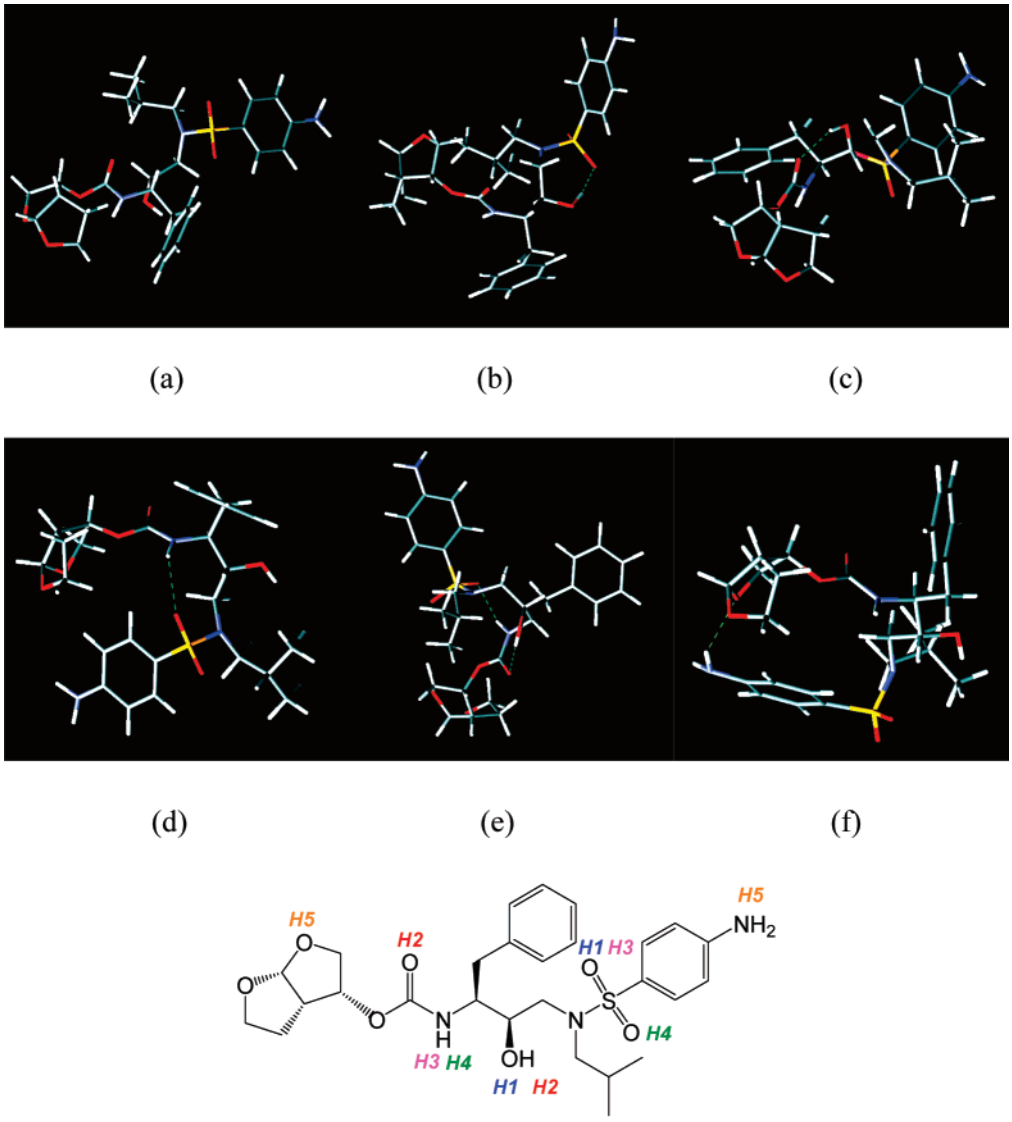

Figure 2. Confwt (a) and five different types of the intramolecular H-bond observed in the gas-phase conformations, illustrated here by conf01 (b; type 1), conf23 (c; type 2), conf06 (d; type 3), conf39 (e; type 4), and conf17 (f; type 5).

fixed for rigid ligand docking. All conformations were submitted to 100 runs of Autodock search which were set to terminate after a maximum of 250 000 energy evaluations or 27 000 generations, yielding 200 docked conformations. The population size was set to 50. The elitism number, the rate of gene mutation, and the rate of gene crossover were 1, 0.02, and 0.8, respectively. The probability that a docking solution in the population would undergo a local search was set to 0.06, and the constraint was set to a maximum of 300 iterations per search. The maximum number of successes or failures before changing the size of local search space (rho), were both set to 4. At the end of a docking job with multiple runs, AutoDock performed a cluster analysis. Docking solutions with ligand all-atom RMSDs within 1.0 Å of each other were clustered together and ranked by the lowest energy representative.

Weblab Viewer Lite, gOpenmol,[52−53] and VMD[54] were used for a graphical interpretation and representation of results.

RESULTS AND DISCUSSION

1. Conformational Searches. The Monte Carlo search resulted in a set of 303 different conformers. The RMSDs of these conformers, compared to the X-ray structure of TMC114 in the wild-type complex, are between 1.5 and 5.2 Å. The conformation of the X-ray structure of TMC114 was not found within these 303 conformers.

In the second step, single point energy calculations of the 303 conformers were performed at the HF/6-31G** level using BRABO. Based on the single point energies, the conformers were divided into 4 groups (Table 1). Then, full (unconstrained) geometry optimizations were performed for a selection of compounds and starting with the 16 compounds in group 1. After the subsequent optimization of the 13 conformers in group 2, one conformer (conf17) was identified with a lower energy than any conformer obtained after optimization of group 1. Optimization of the 14 conformers of the next group (group 3) yielded no conformer having an energy lower than that of conf17. In addition, the lowest

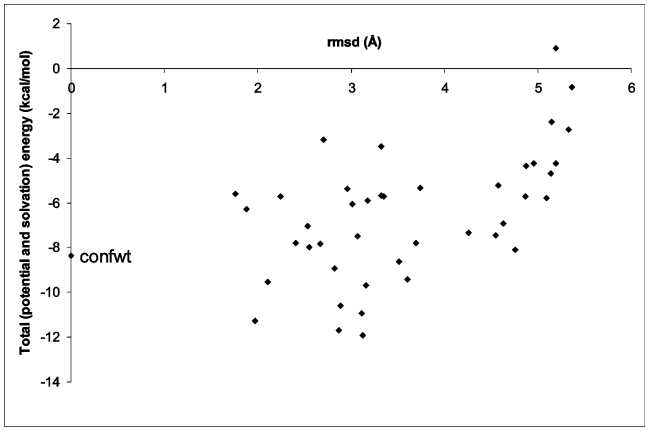

Figure 3. Plot of the rmsd (Å), compared to confwt, of all 43 conformers versus their total (potential and solvation) energies (kcal/mol).

energy obtained for a conformer of group 3 (conf30) is higher than the lowest energy conformer in group 1 (conf01). Due to limited computational resources it was not feasible to perform geometry optimizations for all 303 conformers. Therefore, it was assumed that the most stable conformations of TMC114 are very likely to be present in the three selected groups, and no further conformers were optimized. The results for all 43 conformers that were fully optimized are given in Table 2. The experimental wild-type X-ray structure named "confwt" was also optimized and included in Table 2 for comparison with all calculated conformers.

1.1. Intramolecular H-Bond Interactions. In the 43 conformers obtained after conformational analysis, five types of intramolecular H-bond interactions were observed that are not present in the X-ray structure. Figure 2 shows the structures of conf01, conf23, conf06, conf39, and conf17 as examples of the five different types of intramolecular H-bond, numbered as type 1 through 5, respectively. The first H-bond interaction (H-bond1) is between the −OH group and the −S═O group (Figure 2b). The second H-bond interaction (H-bond2) is between the −OH group and the −C═O group (Figure 2c). The third and the fourth H-bond interaction is between the −NH group and the −S═O group (Figure 2d,e). The fifth H-bond interaction is between the $-NH_2$ of the aniline moiety and one of the oxygen atoms of bis-THF (Figure 2f). From Table 2 it can be seen that H-bond1 is present in more than half of the 43 optimized conformers. The range of the van der Waals surface of the 44 conformers, including confwt, is between 580.5 and 595.1 $Å^2$ with the largest surface area observed for the conformations with no intramolecular H-bond interaction (Table 2). The free energy of solvation of the 44 conformers varies between −5.50 and −15.43 kcal/mol. Confwt has the lowest free energy of solvation (−15.43 kcal/mol), indicating that this conformation is preferred in solution. In the gas phase, on the other hand, it has the next to highest conformational energy. However, when the potential (optimized) energy and the free energy of solvation are combined (Total E, Table 2) we also see that confwt has a lower energy than conf17. Figure 3 shows the plot of the total (solvation and potential) energy versus the rmsd (Å) compared to confwt of all 43 conformers. rmsd correlates not so well with the total energy because of the effect of both the potential energy (intramolecular interactions) and the solvation energy (intermolecular interaction) included in the calculations.

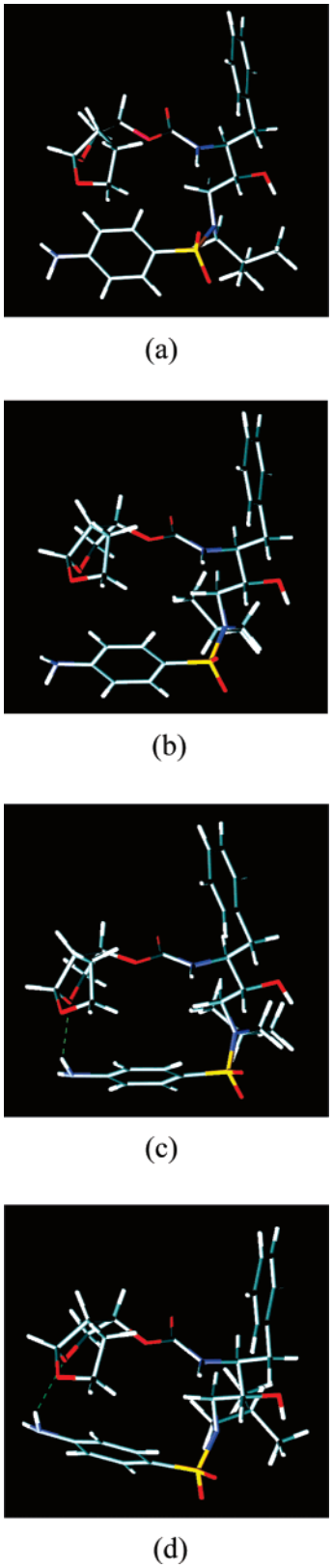

Figure 4. Conf21 (a), conf20 (b), conf04 (c), and conf17 (d).

1.2. Gas-Phase Minimum Energy Conformer. One of the most important differences between the lowest energy gas phase conformer obtained after minimization (conf17; Table 2) and the X-ray structure is an intramolecular H-bond. The aniline moiety in conf17 forms a weak intramolecular H-bond interaction (O...H distance = 2.47 Å, valence angle = 142.4°) with the oxygen of the bis-THF (Figure 2f). As a conse-

Table 3. Relative Conformational Energy (in kcal/mol), H-Bond, RMSD (in Å), and Binding Energy (in kcal/mol) after Rigid Docking of All Conformers That Have a Conformation Similar to the Lowest Energy Conformer, conf17

	gas phase		docked in WT HIV-1 PR		compare docking pose WT vs triple mutant rmsd[c]	docked in triple mutant HIV-1 PR	
	rel energy	H-bond5	rmsd[a]	binding energy		rmsd[b]	binding energy
confwt	7.05	no	0.43	−13.99	0.37	0.47	−13.29
conf21	3.08	no	8.19	−5.27	0.55	8.20	−7.64
conf20	2.78	no	8.27	−2.98	9.45	4.97	−7.21
conf04	1.92	yes	8.16	−0.62	0.42	8.41	−6.09
conf17	0.00	yes	8.25	+6.49	7.07	8.37	−8.06

[a] rmsd between the docked WT complex and the X-ray structure of TMC114 in a complex with the wild-type enzyme. [b] rmsd between the docked triple mutant complex and the X-ray structure of TMC114 in a complex with the triple mutant enzyme. [c] rmsd between the conformation in the docked wild-type and the docked triple mutant complexes.

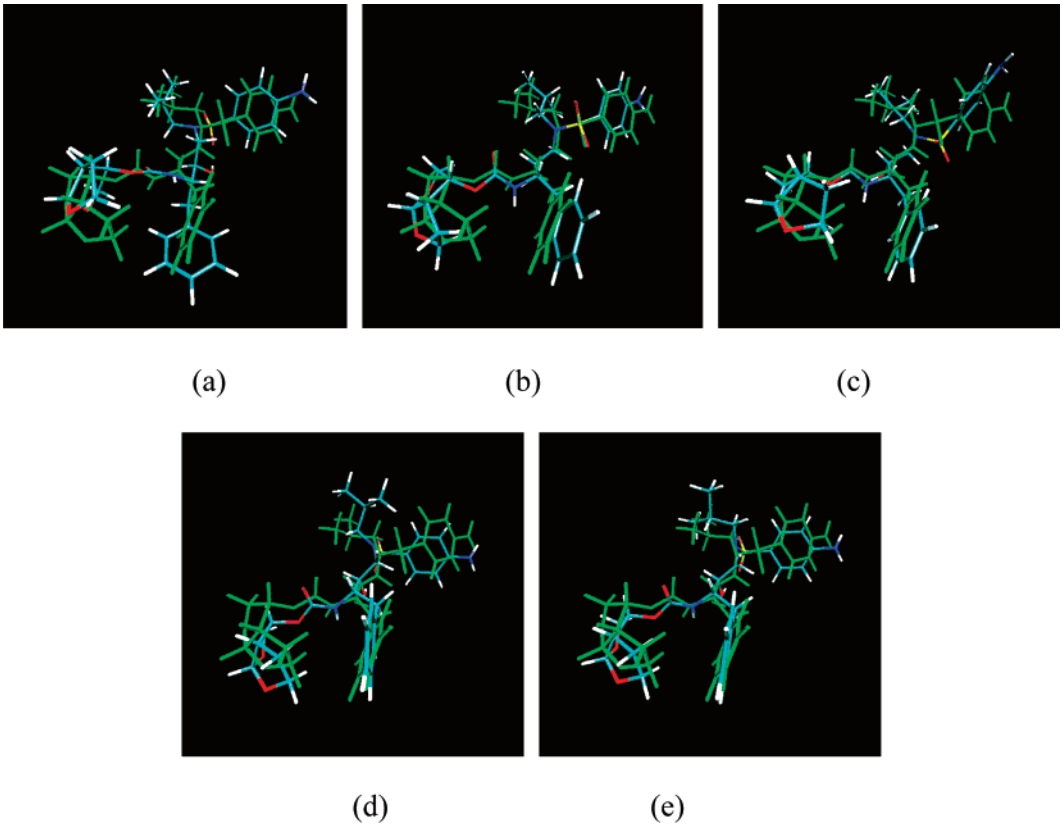

Figure 5. Superposition of the X-ray structure (green) and the optimized structure of conf40 (a), conf35 (b), conf13 (c), conf11 (d), and conf05 (e).

quence, this oxygen atom will not be able to interact with the P2 pocket of the enzyme upon binding. In Figure 4 and Table 3, a detailed comparison of conf17 with similar conformers (conf21, conf20, and conf04) is presented. When only the gas phase (potential) energy is considered, conf04 and conf17 have a lower conformational energy than conf21 and conf20 because of the extra H-bond interaction which stabilizes the structures of conf04 and conf17 in the gas phase. Moreover, it is also shown from the results (see Table 2) that the free energies of solvation of these 4 conformers are between −8.09 and −10.24 kcal/mol which is significantly higher than that of the confwt (−15.43 kcal/mol). This is a consequence of the fact that gas-phase calculations tend to promote the formation of intramolecular hydrogen bonds, but in the solvent or in the enzymatic environment more favorable intermolecular hydrogen bonds can be formed.

1.3. Comparison of All Conformers with the X-ray Structure. In a comparison of all conformers with the optimized X-ray structure, named "confwt", five conformers were identified that have a conformation similar to the X-ray structure: conf40, conf35, conf13, conf11, and conf05 (Figure 5). From Table 4 it can be seen that the relative conformational energies (in the gas phase) of these conformers are always lower than the energy calculated for confwt. Three out of five conformers form a H-bond (type 1) between the hydroxyl and sulfonyl functional groups. For conf13 the rmsd to confwt is the lowest (1.77 Å), but nevertheless the difference in free energy of solvation between these two conformers is quite large (see Table 2). This can be explained by the geometry differences (see Figure 6) of these 2 conformers. Figure 6 shows the water accessible surface of confwt (6a) and conf13 (6b). Conf13 has less contact with

Table 4. Relative Conformational Energy (in kcal/mol), H-Bond, RMSD (in Å), and Binding Energy (in kcal/mol) after Rigid Docking of All Conformers That Have a Conformation Similar to the X-ray Structure

	gas phase		docked in WT HIV-1 PR		compare docking pose WT vs triple mutant rmsd[c]	docked in triple mutant HIV-1 PR	
	rel energy	H-bond5	rmsd[a]	binding energy		rmsd[b]	binding energy
confwt	0.00	no	0.43	−13.99	0.37	0.47	−13.29
conf40	−0.91	yes	8.93	−3.32	8.26	5.16	−4.06
conf35	−1.57	no	1.38	−12.07	0.53	1.37	−11.72
conf13	−2.78	no	9.07	−6.37	0.08	9.08	−5.27
conf11	−4.15	yes	2.99	+9.07	8.92	8.68	+0.78
conf05	−4.98	yes	2.69	−2.78	0.31	2.67	−1.97

[a] rmsd between the docked WT complex and the X-ray structure of TMC114 complexed to the wild-type enzyme. [b] rmsd between the docked triple mutant complex and the X-ray structure of TMC114 complexed to the triple mutant enzyme. [c] rmsd between the conformation in the docked wild-type and the docked triple mutant complexes.

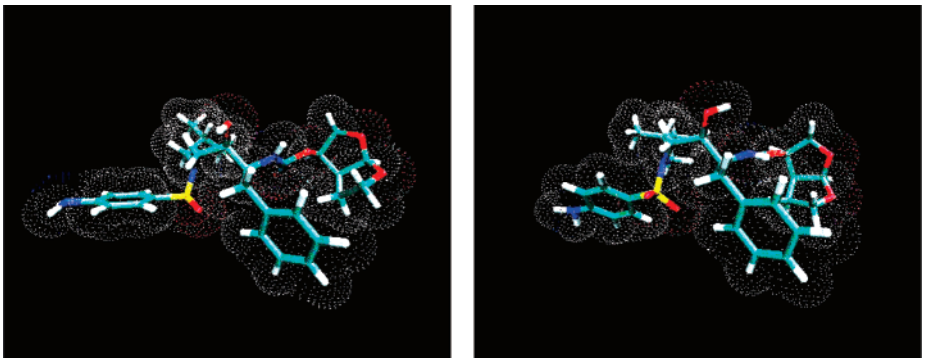

Figure 6. Water accessible surface of confwt (a) and conf13 (b).

the water molecules because the isopropyl and the aminobenzyl groups of conf13 are closer to each other than confwt (see the left-hand side of Figure 6a,b). This is also confirmed in the smaller van der Waals surface for conf13 (Table 2).

2. Docking Calculations. The binding energy after rigid docking in the wild-type and triple mutant HIV-1 PR is included in Tables 3 and 4 for the compounds that are similar to the lowest energy conformation (conf17) and the X-ray conformation (confwt), respectively. Tables 3 and 4 also show the rmsd between the docked wild-type complex and the X-ray structure of TMC114 in a complex with the wild-type enzyme and the rmsd between the docked triple mutant complex and the X-ray structure of TMC114 in a complex with the triple mutant enzyme. In addition, the rmsd between the conformation in the docked wild-type and in the docked triple mutant complexes is also shown. As HIV-1 PR is a homodimer enzyme and the binding pocket is more or less symmetric, compounds can be docked in two different orientations, with the bis-THF of TMC114 binding the P2 pocket in one orientation and the P2′ binding pocket in the other. Also in the X-ray structures these alternate binding modes are observed.[55] In this study, the RMSDs have been calculated with respect to these two alternate X-ray binding modes, and only the lowest rmsd is then presented in Tables 3 and 4. For the conformations presented in Table 3, the rmsd deviations with respect to the wild-type and triple mutant X-ray structures indicate that the binding mode of these conformations is significantly different from the X-ray binding mode. All conformers are renamed as "dconf" instead of "conf" after they were docked into the binding site of HIV-1 PR.

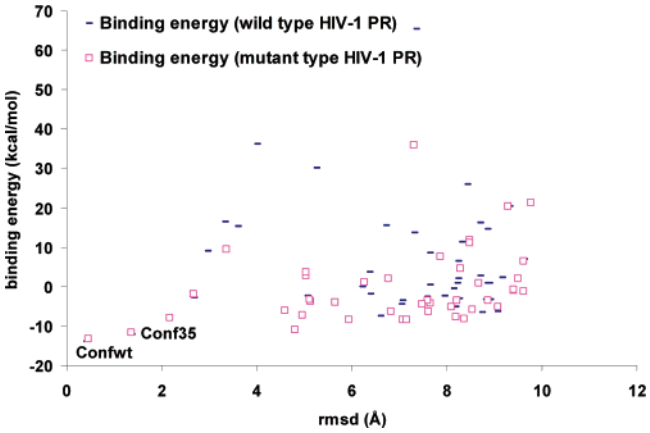

Figure 7. Plot of the rms deviation (Å) (compared with the X-ray structure of TMC114) versus binding energy (kcal/mol) from rigid ligand docking, both the wild-type and a triple mutant (L63P/V82T/I84V) of HIV-1 PR.

The rmsd between the docked wild-type and the docked mutant structure indicates that dconf04 as well as dconf21 is docked in the same pose in the wild-type and the mutant structure, while the poses of dconf20 and dconf17 are completely different in the wild-type and mutant complex. Although the pose in docked wt and docked mutant is very similar for dconf04 and dconf21, the binding energy in the mutant-type HIV-1 PR is better, suggesting that these two conformers bind better to the mutant than the wild-type HIV-1 PR. To compare the strength of the binding energy of these conformers, the binding energy of confwt was also included in Table 3. It is clear that the binding energy is significantly weaker for these 4 conformers compared to confwt.

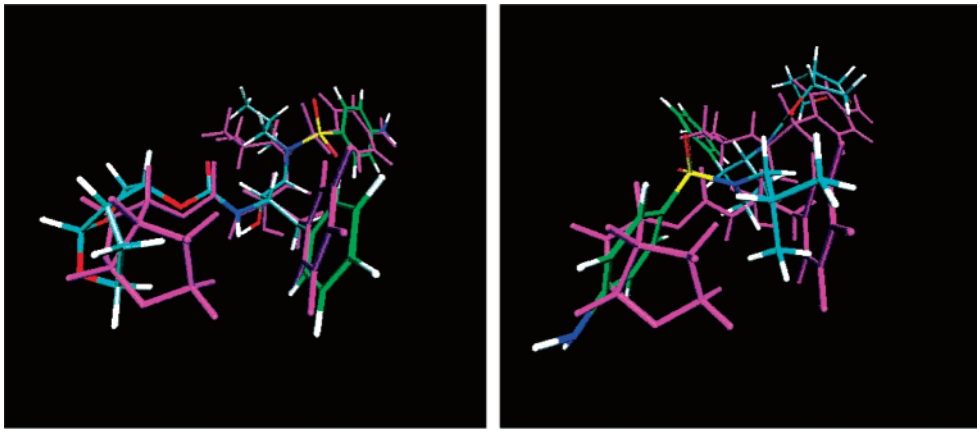

Figure 8. Superposition of the X-ray conformation of TMC114 (magenta) and the two binding modes (a-b) of conf35 after rigid docking into the wild-type of HIV-1 PR.

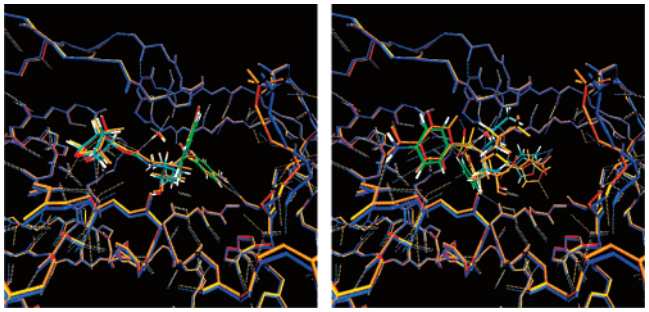

Figure 9. Two binding modes (10a and 10b) of conf35 docked into the wild-type (blue) and a triple mutant (L63P/V82T/I84V) (orange) of HIV-1 PR using rigid ligand docking.

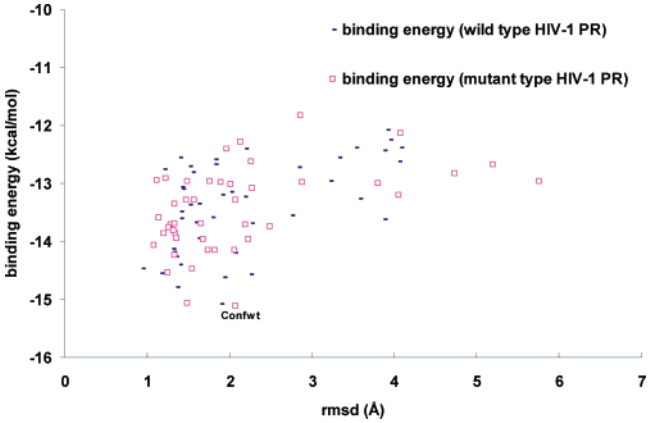

Figure 10. Plot of the rms deviation (Å) (compared with the X-ray structure of TMC114) versus binding energy (kcal/mol) from flexible ligand docking, both the wild-type and a triple mutant (L63P/V82T/I84V) of HIV-1 PR.

For the conformations that are close to the X-ray conformation (Table 4) the binding energy in wild-type HIV-1 PR correlates well with the binding energy in the triple mutant protease for the four conformations with the same docking pose in both protease variants. The rmsd between docked wild-type and mutant-type conformations is large for dconf11 and dconf40, which have a different pose in the wild-type and mutant HIV-1 PR. It can also be observed that the compounds that are not stabilized through an intramolecular H-bond (dconfwt, dconf35, and dconf13) bind better in the binding site of HIV-1 PR, both in the wild-type and the triple mutant (L63P/V82T/I84V), than the other compounds because the former have a free hydroxyl function that can interact with the catalytic site in HIV-1 PR.

The binding energy after rigid docking in wild-type and mutant HIV-1 PR of all 43 conformers is summarized in Figure 7. Figure 7 shows the plot between the binding energy and the rmsd of the conformers compared to the X-ray structure of TMC114 for the wild-type and the mutant-type complexes. The conformations (dconfwt and dconf35) with the lowest rmsd (left-hand side of Figure 7), that are expected to be closer to the 'real' binding mode, bind well to both the wild-type and the mutant proteases. The binding pose of dconf35 is very close to the X-ray structure of TMC114 for both the wild-type and the mutant-type HIV-1 PR (rmsd of 1.38 and 1.37 Å, respectively). When studied in more detail, it was observed that dconf35 binds in the two previously described alternate binding modes both in the wild-type and in the mutant enzyme (Figures 8 and 9) in agreement with the results from Weber et al.[39] The calculated binding energy of dconf35 after rigid docking in the wild-type and the triple mutant HIV-1 PR is −12.07 and −11.72 kcal/mol, respectively, for binding mode A (Figure 9a) and −10.37 and −8.96 kcal/mol, respectively, for binding mode B (Figure 9b).

The binding energy after docking into the wild-type HIV-1 PR does not seem to be correlated with the binding energy after docking into the triple mutant HIV-1 PR (data not shown). The mutations of Val82 to Thr82 and Ile84 to Val84 in the triple mutant HIV-1 PR change the shape of the binding pocket and therefore also the orientation of the inhibitors and the value of the calculated binding energy. Although the gas phase conformational energy of TMC114 is higher in the X-ray conformation compared with the energies of the other conformers, the largest (most negative) calculated binding energy (the energy upon binding the enzyme) was obtained for this wild-type X-ray structure, indicating that this conformation is preferred for binding the active site of HIV-1 PR. The wild-type X-ray structure of TMC114 is also a preferred structure in the binding site of the mutant HIV-1 PR, because of the high similarity (rmsd = 0.1 Å) between the X-ray structures of TMC114 in the wild-type and the mutant protease.

Figure 10 shows the binding energies of the 43 conformers after flexible ligand docking into the wild-type and a triple mutant (L63P/V82T/I84V) HIV-1 PR versus the rmsd with respect to the X-ray structure of TMC114 in the wild-type and the mutant enzymes, respectively. Also after flexible

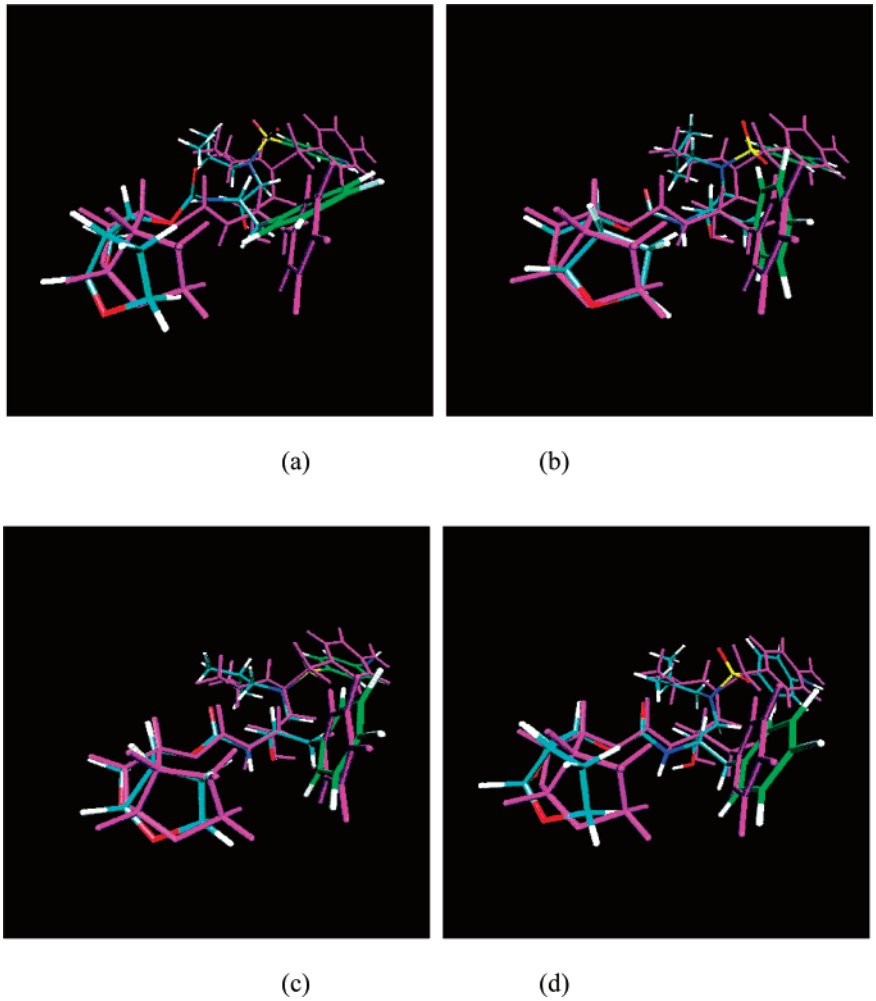

Figure 11. Superposition of TMC114 from the X-ray structure (magenta) and dconf21 (a), dconf05 (b), dconf32 (c), and dconfwt (d) after flexible docking into wild-type HIV-1 PR.

docking, the X-ray conformer is the preferred conformation for binding to both wild-type and mutant HIV-1 PR, and the energy differences are very small (−15.09 and −15.12 kcal/mol for the wild-type and mutant-type, respectively). During the flexible docking procedure, all conformers went through significant conformational changes and most of the conformers are after optimization very similar to the X-ray structure, and the energy differences between the wild-type and the mutant-type of all conformers are between 0.02 and 1.99 kcal/mol. For most structures the same binding mode was obtained, in which the bis-THF of TMC114 binds at the P2 binding pocket. For the docked conformers dconf26 and dconf34 in the wild-type HIV-1 PR and dconf19, dconf22, dconf26, dconf34, and dconf43 in the mutant-type HIV-1 PR, the second binding mode was observed, in which the bis-THF of TMC114 binds at the P2′ binding pocket. Although many of the conformations obtained after flexible docking reside in different local minima in conformational space, the binding energy to the enzyme is in the same range, varying between −15 and −12 kcal/mol. This indicates that the compound is able to adapt to conformational changes in the binding pocket without large energy penalty. In addition, Figure 10 illustrates that the conformational differences between the results of the different flexible docking calculations can be very large. In principle, if sufficient conformational sampling is performed for each starting conformation, each run should produce the same complex close to the global minimum. In practice, however, this would take too much computational resources.

In Figure 11 the four conformations (dconf21, dconf05, dconf32, and dconfwt) with the lowest binding free energies in wild-type HIV-1 PR are shown and superimposed on the X-ray structure. It can be seen that they are structurally very similar to the X-ray structure. For these conformations the detailed intermolecular interactions are compared to the X-ray structure in Table 5. Table 5 shows the H-bond interactions between the inhibitor and Asp25′, Asp29, Asp30, Asp30′ and the flap water molecule (that interacts with the backbone of Ile50 and Ile50′). These interactions play an important role in the binding of TMC114 to HIV-1 PR. It can be seen from the results that most of the distances of H-bond interactions are less than 2.50 Å, and the results from dconf21, dconf05, dconf32 and dconfwt are very close to the result from the X-ray structure.

This conformational study shows the importance of the flexibility of TMC114 (Table 5). The different H-bonds between TMC114 and the amino acids of HIV-1 PR or water molecules that can be formed constitute the stability of TMC114 because they can compensate for each other leading to an overall strong interaction. For example, dconf21 is one of the most stable conformers because it has stronger interactions between Asp 30 (−NH) ... Inh (O2**) (1.68 Å)

Table 5. H-Bond Interactions (Å) between TMC114 and HIV-1 PR Obtained after Flexible Ligand Docking into the Binding Site of Wild-Type HIV-1 PR[a]

H-bonds	dconf21	dconf05	dconf32	dconfwt	X-ray
Asp 25′ (−C═O) ... Inh (−OH)	none[c]	1.98	2.41	2.13	1.58
Asp 29 (−NH) ... Inh (O1[b])	2.31	2.11	1.99	1.90	1.95
Asp 30 (−NH) ... Inh (O2[b])	1.68	2.00	1.83	1.86	2.07
Asp 30′ (−C═O) ... Inh (−NH)	2.19	2.15	none[c]	2.23	2.06
flap water (−OH)... Inh (−C═O)	2.11	3.17	2.06	1.85	1.80
flap water (−OH)... Inh (−S═O)	1.93	2.49	2.40	2.49	2.02

[a] The distances of the H-bonds are measured between the hydrogen atoms of the hydrogen bridge and the acceptor atoms. [b] The oxygen atom of the bis-tetrahydrofuranyl (bis-THF) group of TMC114. [c] none = no H-bond interaction.

and flap water (−OH)... Inh (−S═O) (1.93 Å) than that of the X-ray structure, while the other interactions are poorer than the X-ray structure.

CONCLUSIONS

The conformational analysis of TMC114, a potent inhibitor of HIV-1 PR, yielded 43 conformers in which five types of intramolecular H-bond interactions could be identified which are not present in the X-ray structure. In order to compare the strength of the intramolecular H-bond interactions of all 43 conformations, the full geometry optimizations of these conformations were performed and their energies were calculated using ab initio molecular orbital calculations at the Hartree−Fock (HF) level with the 6-31G** basis set. The lowest energy conformer is different from the X-ray structure because of such an intramolecular H-bond between the $-NH_2$ group of the aniline moiety and the bis-THF oxygen atom. This is a consequence of the fact that gas-phase calculations tend to promote the formation of intramolecular hydrogen bonds but in the solvent or in the enzymatic environment more favorable intermolecular hydrogen bonds can be formed. Therefore, the gas-phase calculations should only be used to sample the conformational space of the molecule, but they should not be used as a predictor for the conformation in the binding pocket.

All 43 conformers were subject to rigid and flexible ligand docking in both wild-type and a triple mutant (L63P/V82T/I84V) HIV-1 PR. Some conformations were observed to dock in two alternative binding modes as a consequence of the nearly symmetric nature of the binding site in this homodimeric enzyme. Also in X-ray structures, these alternative binding orientations have been observed.

Obviously, the results from this study also show that flexible ligand docking is a better approach than rigid ligand docking: the inhibitor needs to adapt itself in order to bind well to the enzyme. The most favorable binding energies were observed for conformations that are very similar to the X-ray structure. It was also observed that due to limited sampling in the flexible docking calculations, the final docking solution depends on the starting conformation of the docking run. However, since enough different starting conformations—based on the QM calculations—were used, we can assume that the conformational space was sampled sufficiently to obtain reliable results.

This conformational flexibility, combined with the crucial binding mode focusing on backbone interactions, allows TMC114 to make a highly stable complex with the protease which leads to less sensitivity of the biological activity and which, more efficient than the other inhibitors,[25] results in continued enzyme inhibition in the presence of several mutations.

ACKNOWLEDGMENT

The authors thank Dr. Herman Van Vlijmen for helpful discussions. The authors acknowledge support from the IWT − Flemish region under grant no. IWT-161. The University of Antwerp is gratefully acknowledged for support under grant BOF UA/SFO UIA 2002 as well as for access to the university's supercomputer cluster CalcUA.

REFERENCES AND NOTES

(1) Wlodawer, A.; Vondrasek, J. Inhibitors of HIV-1 protease: a major success of structure-assisted drug design. *Annu. Rev. Biophys. Biomol. Struc.* **1998**, *27*, 249−284.
(2) Wlodawer, A.; Erickson, J. W. Structure-based inhibitors of HIV-1 protease. *Annu. Rev. Biochem.* **1993**, *62*, 543−585.
(3) Patick, A. K.; Potts, K. E. Protease inhibitors as antiviral agents. *Clin. Microbiol. Rev.* **1998**, *11*, 614−627.
(4) De Benedetti, P. G. Molecular modeling and quantitative structure-activity analysis of antibacterial sulfanilamides and sulfones. *Prog. Drug. Res.* **1991**, *36*, 361−417.
(5) Cushman, M.; Golebiewski, W. M.; Pommier, Y.; Mazumder, A.; Reymen, D.; De Clercq, E.; Graham, L.; Rice, W. G. Cosalane analogues with enhanced potencies as inhibitors of HIV-1 protease and integrase. *J. Med. Chem.* **1995**, *38*, 443−452.
(6) Chatfield, D. C.; Brooks, B. R. HIV-1 protease cleavage mechanism elucidated with molecular dynamics simulation. *J. Am. Chem. Soc.* **1995**, *117*, 5561−5572.
(7) De Clercq, E. Toward improved anti-HIV chemotherapy: Therapeutic strategies for intervention with HIV infections. *J. Med. Chem.* **1995**, *38*, 2491−2517.
(8) Eurenius, K. P.; Chatfield, D. C.; Hodoscek, M.; Brooks, B. R. Studying enzyme mechanism with hybrid quantum mechanical and molecular mechanical potentials. I. Theoretical considerations. *Int. J. Quantum Chem.* **1996**, *60*, 1189−1200.
(9) Mavri, J. Irreversible inhibition of the HIV-1 protease: a theoretical study. *Int. J. Quantum Chem.* **1998**, *69*, 753−759.
(10) Kulkarni, S. S.; Kulkarni, V. M. Structure based prediction of binding affinity of human immunodeficiency virus-1 protease inhibitors. *J. Chem. Inf. Comput. Sci.* **1999**, *39*, 1128−40.
(11) Jayatilleke, P. R.; Nair, A. C.; Zauhar, R.; Welsh, W. J. Computational studies on HIV-1 protease inhibitors: Influence of calculated inhibitor-enzyme binding affinities on the statistical quality of 3D-QSAR CoMFA models. *J. Med. Chem.* **2000**, *43*, 4446−51.
(12) Wang, W.; Kollman, P. A. Computational study of protein specificity: The molecular basis of HIV-1 protease drug resistance. *Proc. Natl. Acad. Sci. U.S.A.* **2001**, *98*, 14937−42.
(13) Nair, A. C.; Jayatilleke, P.; Wang, X.; Miertus, S.; Welsh, W. J.; Computational studies on tetrahydropyrimidine-2-one HIV-1 protease inhibitors: Improving three-dimensional quantitative structure-activity relationship comparative molecular field analysis models by inclusion of calculated inhibitor and receptor based properties. *J. Med. Chem.* **2002**, *45*, 973−83.
(14) Meek, T. D. Inhibitors of HIV-1 protease. *J. Enzyme Inhib.* **1992**, *6*, 65−98.
(15) Kempf, D. J.; Marsh, K. C.; Denissen, J. F.; McDonald, E.; Vasavanonda, S.; Flentge, C. A.; Green, B. E.; Fino, L.; Park, K. C.; Kong, X.; Wideburg, N. E.; Saldvar, A.; Ruiz, L.; Kati, W. M.; Sham, H. L.; Robins, T.; Stewart, K. D.; Hsu, A.; Plattner, J. J.; Leonard, J.

M.; Norbeck, D. W. ABT-538 is a potent inhibitor of human immunodeficiency virus protease and has high oral bioavailability in humans. *Proc. Natl. Acad. Sci. U.S.A.* **1995**, *92*, 2484−2488.
(16) Kempf, D. J.; Sham, H. L.; Marsh, K. C.; Flentge, C. A.; Betebenner, D.; Green, B. E.; McDonald, E.; Vasavanonda, S.; Saldivar, A.; Wideburg, N. E.; Kati, W. M.; Ruiz, L.; Zhao, C.; Fino, L.; Patterson, J.; Molla, A.; Plattner, J. J.; Norbeck, D. W. Discovery of ritonavir, a potent inhibitor of HIV protease with high oral bioavailability and clinical efficacy. *J. Med. Chem.* **1998**, *41*, 602−617.
(17) Roberts, N. A.; Martin, J. A.; Kinchington, D.; Broadhurst, A. V.; Craig, J. C.; Duncan, I.; Galpin, S. A.; Handa, B. K.; Kay, J.; Krohn, A.; Lambert, R. W.; Merrett, J. H.; Mills, J. S.; Parkes, K. E. B.; Redshaw, S.; Ritchie, A. J.; Taylor, D. L.; Thomas, G. L.; Mchain, P. J. Rational design of peptide-based HIV proteinase inhibitors. *Science* **1990**, *248*, 358−361.
(18) Dreyer, G. B.; Metcalf, B. W.; Tomaszek, T. A., Jr.; Carr, T. J.; Chandler, A. C., III; Hyland, L.; Fakhoury, S. A.; Magaard, V. W.; Moore, M. L.; Strickler, J. E.; Debouck, C.; Meek, T. D. Inhibition of human immunodeficiency virus 1 protease in vitro: rational design of substrate analogue inhibitors. *Proc. Natl. Acad. Sci. U.S.A.* **1989**, *86*, 9752−9756.
(19) Vacca, J. P.; Dorsey, B. D.; Schleif, W. A.; Levin, R. B.; McDaniel, S. L.; Darke, P. L.; Zugay, J.; Quintero, J. C.; Blahy, O. M.; Roth, E.; Sardana, V. V.; Schlabach, A. J.; Graham, P. I.; Condra, J. H.; Gotlib, L.; Holloway, M. K.; Lin, J.; Chen, I.; Vastag, K.; Ostovic, D.; Anderson, P. S.; Emini, E. A.; Huff, J. R. L-735,524: An orally bioavailable human immunodeficiency virus type 1 protease inhibitor. *Proc. Natl. Acad. Sci. U.S.A.* **1994**, *91*, 4096−4100.
(20) James, J. S. Birmingham UK drug therapy conference−early report. *AIDS Treat. News* **1996**, *259*, 1−2.
(21) Kaldor, S. W.; Kalish, V. J.; Davies, J. F., 2nd; Shetty, B. V.; Fritz, J. E.; Appelt, K.; Burgess, J. A.; Campanale, K. M.; Chirgadze, N. Y.; Clawson, D. K.; Dressman, B. A.; Hatch, S. D.; Khalil, D. A.; Kosa, M. B.; Lubbehusen, P. P.; Muesing, M. A.; Patick, A. K.; Reich, S. H.; Su, K. S.; Tatlock, J. H. Viracept (Nelfinivir mesylate, AG1343): A potent, orally bioavailable inhibitor of HIV-1 protease. *J. Med. Chem.* **1997**, *40*, 3979−3985.
(22) Rocheblave, L.; Bihel, F.; De Michelis, C.; Priem, G.; Courcambeck, J.; Bonnet, B.; Chermann, J.-C.; Kraus, J.-L. Synthesis and antiviral activity of new anti-HIV amprenavir bioisosteres. *J. Med. Chem.* **2002**, *45*, 3321−3324.
(23) D'Aquila, R. T. Drug resistance mutations in HIV-1. *Top HIV Med.* **2003**, *11*, 92−96.
(24) Surleraux, D. L.; Tahri, A.; Verschueren, W. G.; Pille, G. M.; De Kock, H. A.; Jonckers, T. H.; Peeters, A.; De Meyer, S.; Azijn, H.; Pauwels, R.; De Bethune, M. P.; King, N. M.; Prabu-Jeyabalan, M.; Schiffer, C. A.; Wigerinck, P. B. Discovery and selection of TMC114, a next generation HIV-1 Protease inhibitor. *J. Med. Chem.* **2005**, *48*, 1813−1822.
(25) King, N. M.; Prabu-Jeyabalan, M.; Nalivaika, E. A.; Wigerinck, P.; de Béthune, M-P.; Schiffer, C. A. Structural and thermodynamic basis for the binding of TMC114, a next-generation human immunodeficiency virus type 1 protease inhibitor. *J. Virol.* **2004**, *78*, 12012−12021.
(26) Kirkpatrick, S.; Gellatt, C. D.; Vecchi, M. P. Optimization by simulated annealing. *Science* **1983**, *220*, 671−680.
(27) Wilson, S. R.; Cui, W.; Moskowitz, J. W.; Schmidt, K. E. Applications of simulated annealing to the conformational analysis of flexible molecules. *J. Comput. Chem.* **1991**, *12*, 342−349.
(28) Nayeem, A.; Vila, J.; Scheraga, H. A. A comparative study of the simulated-annealing and Monte Carlo-with-minimization approaches to the minimum-energy structures of polypeptides: [met]-enkephalin. *J. Comput. Chem.* **1991**, *12*, 594−605.
(29) Shenkin, P. S.; Yarmush, D. L.; Fine, R. M.; Wang, H.; Levinthal, C. Predicting antibody hypervariable loop conformations II: Minimization and molecular dynamics studies of MCPC603 from many randomly generated loop conformations. *Proteins: Struct., Funct., Genet.* **1986**, *1*, 342−362.
(30) Shenkin, P. S.; Yarmush, D. L.; Fine, R. M.; Wang, H.; Levinthal, C. Predicting antibody hypervariable loop conformation. I. ensembles of random conformations for ringlike structures. *Biopolymers* **1987**, *26*, 2053−2085.
(31) Chang, G.; Guida, W. C.; Still, W. C. An Internal Coordinate Monte Carlo Method for Searching Con formational Space. *J. Am. Chem. Soc.* **1989**, *111*, 4379−4386.
(32) Weinberg, N.; Wolfe, S. A. A comprehensive approach to the conformational analysis of cyclic compounds. *J. Am. Chem. Soc.* **1994**, *116*, 9860−9868.
(33) Li, Z.; Scheraga, H. A. Monte Carlo-minimization approach to the multiple-minima problem in protein folding. *Proc. Natl. Acad. Sci. U.S.A.* **1987**, *84*, 6611−6615.
(34) Freyberg, B. V.; Braun, W. Efficient search for all low energy conformations of polypeptides by monte carlo methods. *J. Comput. Chem.* **1991**, *12*, 1065−1076.
(35) Kolossvary, I.; Guida, W. C. Low mode search. an efficient, automated computational method for conformational analysis: application to cyclic and acyclic alkanes and cyclic peptides. *J. Am. Chem. Soc.* **1996**, *118*, 5011−5019.
(36) Kolossvary, I.; Guida, W. C. Low-mode conformational search elucidated: application to $C_{39}H_{80}$ and flexible docking of 9-deaza-guanine inhibitors into PNP. *J. Comput. Chem.* **1999**, *20*, 1671−1684.
(37) Kolossvary, I.; Keseru, G. Hessian-free low-mode conformational search for large-scale protein loop optimization: application to c-jun N-terminal kinase JNK3. *J. Comput. Chem.* **2001**, *22*, 21−30.
(38) Trylska, J.; Bala, P.; Geller, M.; Grochowski, P. Molecular dynamics simulations of the first steps of the reaction catalyzed by HIV-1 protease. *Biophys. J.* **2002**, *83*, 794−807.
(39) Van Gunsteren, W. F.; Berendsen, H. J. C. Computer simulation of molecular dynamics: methodology, applications and perspectives in chemistry. *Angew. Chem., Int. Ed. Engl.* **1990**, *29*, 992−1023.
(40) Boresch, S.; Karplus, M. The meaning of component analysis: decomposition of the free energy in terms of specific interactions. *J. Mol. Biol.* **1995**, *254*, 801−807.
(41) Hansson, T.; Oostenbrink, C.; Van Gunsteren. W. F. Molecular dynamics simulations. *Curr. Opin. Struct. Biol.* **2002**, *12*, 190−196.
(42) Florián, J.; Warshel, A. Langevin dipoles model for *ab initio* calculations of chemical processes in solution: Parametrization and application to hydration free energies of neutral and ionic solutes, and conformational analysis in aqueous solution. *J. Phys. Chem. B* **1997**, *101*, 5583−5595.
(43) Bren, U.; Martínek, V.; Florián, J. Decomposition of the solvation free energies of deoxyribonucleoside triphosphates using the free energy perturbation method. *J. Phys. Chem. B* **2006**, *110*, 12782 − 12788.
(44) Petersson, G. A.; Bennett, A.; Tensfeldt, T. G.; Al-Laham, M. A.; Shirley, W. A.; Mantzaris, J. A complete basis set model chemistry. I. The total energies of closed-shell atoms and hydrides of the first-row elements. *J. Chem. Phys.* **1988**, *89*, 2193−2218.
(45) Petersson, G. A.; Al-Laham, M. A. A complete basis set model chemistry. II. Open-shell systems and the total energies of the first-row atoms. *J. Chem. Phys.* **1991**, *94*, 6081−6091.
(46) Van Alsenoy, C.; Peeters, A. BRABO: a program for ab initio studies on large molecular systems. *J. Mol. Struct. (Theochem)* **1993**, *286*, 19−34.
(47) Cancès, M. T.; Mennucci, B.; Tomasi, J. A new integral equation formalism for the polarizable continuum model: theoretical background and applications to isotropic and anisotropic dielectrics. *J. Chem. Phys.* **1997**, *107*, 3032−3041.
(48) Pedretti, A.; Villa, L.; Vistoli, G. VEGA: a versatile program to convert, handle and visualize molecular structure on Windows-based PCs. *J. Mol. Graphics Modell.* **2002**, *21*, 47−49.
(49) Morris, G. M.; Goodsell, D. S.; Halliday, R. S.; Huey, R.; Hart, W. E.; Belew, R. K.; Olson, A. J. Automated docking using a Lamarckian genetic algorithm and an empirical binding free energy function. *J. Comput. Chem.* **1998**, *19*, 1639−1662.
(50) Weiner, S. J.; Kollman, P. A.; Case, D. A.; Singh, U. C.; Ghio, C.; Alagona, G.; Profeta, S.; Weiner, P. A. New force field for molecular mechanical simulation of nucleic acids and proteins. *J. Am. Chem. Soc.* **1984**, *106*, 765−784.
(51) Halgren, T. Maximally diagonal force constants in dependent angle-bending coordinates. II. Implications for the design of empirical force fields. *J. Am. Chem. Soc.* **1990**, *112*, 4710−4723.
(52) Laaksonen, L. A graphics program for the analysis and display of molecular dynamics trajectories. *J. Mol. Graphics Modell.* **1992**, *10*, 33−34.
(53) Bergman, D. L.; Laaksonen, L.; Laaksonen, A. Visualization of solvation structures in liquid mixtures. *J. Mol. Graphics Modell.* **1997**, *15*, 301−306.
(54) Humphrey, W.; Dalke, A.; Schulten, K. VMD-Visual Molecular Dynamics. *J. Mol. Graphics Modell.* **1996**, *14*, 33−38.
(55) Tie, Y.; Boross, P. I.; Wang, Y.; Gaddis, L.; Hussain, A. K.; Leshchenko, S.; Ghosh, A. K.; Louis, J. M.; Harrison, R. W.; Weber, I. T. High resolution crystal structures of hiv-1 protease with a potent non-peptide inhibitor (uic-94017) active against multi-drug resistant clinical strains. *J. Mol. Biol.* **2004**, *338*, 341−352.

CI7001318